Compressible fiber optic micro-Fabry-Pérot cavity with ultra-high pressure sensitivity

Ying Wang,[1,2] D. N. Wang,[1,*] Chao Wang,[1] and Tianyi Hu[1]

[1]*Department of Electrical Engineering, The Hong Kong Polytechnic University, Hong Kong, China*
[2]*Laboratory of Optical Information Technology and School of Science, Wuhan Institute of Technology, 430073, Wuhan, China*
[*]*eednwang@polyu.edu.hk*

Abstract: We propose and demonstrate a pressure sensor based on a micro air bubble at the end facet of a single mode fiber fusion spliced with a silica tube. When immersed into the liquid such as water, the air bubble essentially acts as a Fabry-Pérot interferometer cavity. Such a cavity can be compressed by the environmental pressure and the sensitivity obtained is >1000 nm/kPa, at least one order of magnitude higher than that of the diaphragm-based fiber-tip sensors reported so far. The compressible Fabry-Pérot interferometer cavity developed is expected to have potential applications in highly sensitive pressure and/or acoustic sensing.

OCIS codes: (060.2370) Fiber optics sensors; (120.0120) Instrumentation, measurement, and metrology; (120.2230) Fabry-Perot.

References and links

1. M. Xu, L. Reekie, Y. Chow, and J. P. Dakin, "optical in-fibre grating high pressure sensor," Electron. Lett. **29**(4), 398–399 (1993).
2. D. Chen, G. Hu, and L. Chen, "Dual-core photonic crystal fiber for hydrostatic pressure sensing," IEEE Photon. Technol. Lett. **23**(24), 1851–1853 (2011).
3. C. Wu, H. Y. Fu, K. K. Qureshi, B.-O. Guan, and H. Y. Tam, "High-pressure and high-temperature characteristics of a Fabry-Perot interferometer based on photonic crystal fiber," Opt. Lett. **36**(3), 412–414 (2011).
4. Z. Liu, M.-L. V. Tse, C. Wu, D. Chen, C. Lu, and H. Y. Tam, "Intermodal coupling of supermodes in a twin-core photonic crystal fiber and its application as a pressure sensor," Opt. Express **20**(19), 21749–21757 (2012).
5. T. W. Kao and H. F. Taylor, "High-sensitivity intrinsic fiber-optic Fabry-Perot pressure sensor," Opt. Lett. **21**(8), 615–617 (1996).
6. S. Avino, J. A. Barnes, G. Gagliardi, X. Gu, D. Gutstein, J. R. Mester, C. Nicholaou, and H.-P. Loock, "Musical instrument pickup based on a laser locked to an optical fiber resonator," Opt. Express **19**(25), 25057–25065 (2011).
7. H. Y. Choi, K. S. Park, S. J. Park, U.-C. Paek, B. H. Lee, and E. S. Choi, "Miniature fiber-optic high temperature sensor based on a hybrid structured Fabry-Perot interferometer," Opt. Lett. **33**(21), 2455–2457 (2008).
8. G. Gagliardi, M. Salza, S. Avino, P. Ferraro, and P. De Natale, "Probing the ultimate limit of fiber-optic strain sensing," Science **330**(6007), 1081–1084 (2010).
9. J. H. Chow, D. E. McClelland, M. B. Gray, and I. C. M. Littler, "Demonstration of a passive subpicostrain fiber strain sensor," Opt. Lett. **30**(15), 1923–1925 (2005).
10. Y. Wang, D. N. Wang, C. R. Liao, T. Hu, J. Guo, and H. Wei, "Temperature-insensitive refractive index sensing by use of micro Fabry-Pérot cavity based on simplified hollow-core photonic crystal fiber," Opt. Lett. **38**(3), 269–271 (2013).
11. A. Wang, H. Xiao, J. Wang, Z. Wang, W. Zhao, and R. G. May, "Self-calibrated interferometric-intensity-based optical fiber sensors," J. Lightwave Technol. **19**(10), 1495–1501 (2001).
12. Y. Zhu and A. Wang, "Miniature fiber-optic pressure sensor," IEEE Photon. Technol. Lett. **17**(2), 447–449 (2005).
13. D. Donlagic and E. Cibula, "All-fiber high-sensitivity pressure sensor with SiO_2 diaphragm," Opt. Lett. **30**(16), 2071–2073 (2005).
14. X. Wang, J. Xu, Y. Zhu, K. L. Cooper, and A. Wang, "All-fused-silica miniature optical fiber tip pressure sensor," Opt. Lett. **31**(7), 885–887 (2006).
15. W. Wang, N. Wu, Y. Tian, C. Niezrecki, and X. Wang, "Miniature all-silica optical fiber pressure sensor with an ultrathin uniform diaphragm," Opt. Express **18**(9), 9006–9014 (2010).
16. E. Cibula, S. Pevec, B. Lenardič, É. Pinet, and D. Donlagic, "Miniature all-glass robust pressure sensor," Opt. Express **17**(7), 5098–5106 (2009).
17. H. Bae and M. Yu, "Miniature Fabry-Perot pressure sensor created by using UV-molding process with an optical fiber based mold," Opt. Express **20**(13), 14573–14583 (2012).

#187405 - $15.00 USD Received 19 Mar 2013; revised 21 May 2013; accepted 25 May 2013; published 5 Jun 2013

18. F. Guo, T. Fink, M. Han, L. Koester, J. Turner, and J. Huang, "High-sensitivity, high-frequency extrinsic Fabry-Perot interferometric fiber-tip sensor based on a thin silver diaphragm," Opt. Lett. **37**(9), 1505–1507 (2012).
19. F. Xu, D. Ren, X. Shi, C. Li, W. Lu, L. Lu, L. Lu, and B. Yu, "High-sensitivity Fabry-Perot interferometric pressure sensor based on a nanothick silver diaphragm," Opt. Lett. **37**(2), 133–135 (2012).
20. J. Ma, W. Jin, H. L. Ho, and J. Y. Dai, "High-sensitivity fiber-tip pressure sensor with graphene diaphragm," Opt. Lett. **37**(13), 2493–2495 (2012).

1. Introduction

Pressure sensing is one of the most important applications of fiber optic devices in industrial and environmental safety monitoring. Various types of fiber optic pressure sensors have been demonstrated to fulfill specific pressure applications, including fiber Bragg gratings (FBGs) [1], photonic crystal fiber (PCF) devices [2] and interferometers [3, 4], and the pressure sensitivity achieved is typically on the order of −10 pm/Mpa. Among above mentioned configurations, the pressure sensors that are based on Fabry-Pérot (FP) interferometer have shown promising results for static and dynamic pressure measurements [5, 6], as well as other physical and chemical parameter detections such as temperature [7], strain [8, 9] and refractive index [10]. The FP interferometers can achieve extremely high sensitivity and flexibly demodulated in the wavelength domain [3, 4] and frequency domain [6, 8], or simply use light intensity detection [11].

For static pressure sensing with high sensitivity, micro-FP cavity built at the optical fiber end has been investigated intensively. A pressure sensor based on micro FP cavity commonly uses an elastic diaphragm at the fiber tip such as SiO_2/silica, polymer, silver and graphene film [12–20]. The pressure sensitivity of the diaphragm-based fiber tip FP sensor is defined as the ratio of the FP cavity length variation to the pressure change, which critically depends on the size and the mechanical quality of the diaphragm employed. While a silver diaphragm with diameter of 125 μm exhibits a sensitivity of 70.5 nm/kPa [19], a highly elastic graphene diaphragm with diameter of 25 μm has a sensitivity of 39.4 nm/kPa [20]. Obviously, the small size of diaphragm in a miniaturized sensor head imposes a limit on its sensitivity.

Here we propose and demonstrate a diaphragm-free construction of fiber-tip FP cavity sensor that breaks the sensitivity limitations imposed by the transversal dimensions of diaphragm in traditional FP pressure sensors. The sensor proposed here exhibits sensitivity of >15 nm/kPa at around 1550 nm with a wavelength interrogation scheme. Compared to the diaphragm-based sensors, extremely high sensitivity of >1000 nm/kPa can be readily achieved with this method, at least one order of magnitude higher than that of the diaphragm-based fiber-tip sensor reported so far [19, 20].

2. Principle of the compressible FP cavity sensor

By immersing a single mode fiber (SMF) fusion spliced with a section of silica tube into liquid, as shown in Fig. 1(a), a micro air bubble is naturally formed by the capillary effect at the end facet of the SMF. The air-liquid interface acts as a light reflector which, together with the air-SMF interface, forms an FP interferometer (FPI). The length (or the volume) of the FP cavity is highly sensitive to the environmental pressure. As air can be treated as the ideal gas in the pressure range between 1 and 10 bar (1 bar = 100 kPa), the behavior of the air bubble can be described by the well-known ideal gas law as:

$$PV = nRT \tag{1}$$

where P, V and T are the pressure, volume and thermodynamic temperature (in K) of air in the FP cavity, respectively, n is the amount of substance of air, and R is the ideal gas constant (8.31 $J \cdot K^{-1} \cdot mol^{-1}$). The geometry of the air bubble in the FP cavity can be considered as a cylinder, with initial length of L_0 at normal pressure (~1 bar) and diameter of D (the same as the inner diameter of the silica tube). Thus its volume can be calculated as: $V = \pi D^2 L / 4$. By assuming an isothermal process and substituting volume V in Eq. (1), the pressure sensitivity of the compressible FP cavity can be derived as:

#187405 - $15.00 USD Received 19 Mar 2013; revised 21 May 2013; accepted 25 May 2013; published 5 Jun 2013

$$\frac{dL}{dP} = -\frac{P_0 L_0}{P^2} \tag{2}$$

where L is the cavity length under pressure P, and $P_0 = 1$ bar is the normal pressure. It can be seen from Eq. (2) that the pressure sensitivity of the compressible FP cavity only depends on the initial cavity length and the pressure applied, and is independent of inner diameter of the silica tube, which breaks the limit imposed by the diaphragm-based sensors. With an initial cavity length of $L_0 = 100$ μm, the pressure sensitivity of such a device is estimated to be −1000 nm/kPa at normal pressure. While for higher pressure operation, the sensitivity is still as high as −40 nm/kPa at 5 bar.

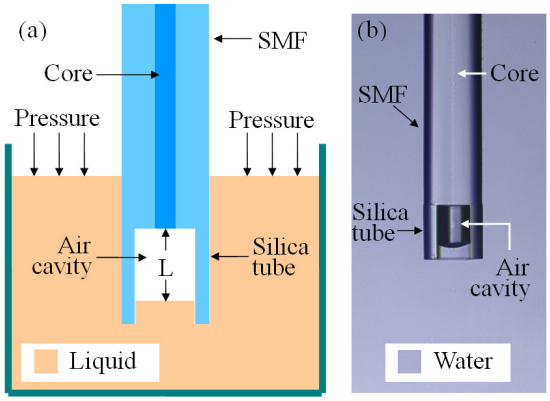

Fig. 1. (a) Schematic diagram and (b) microscopic image of the compressible micro FP cavity. The lengths of the silica tube and air cavity in (b) are 114 and ~90 μm, respectively.

3. Experiment results and discussion

In our experiments, a silica tube with inner/outer diameter of 75/127μm was used. The silica tube was fusion spliced with conventional SMFs (SMF-28e, Corning) and then cleaved at a position of tens of micrometers away from the splicing joint. The open air cavity in the silica tube was subsequently immersed into water which was filled into the tube due to capillary effect and as a result, an enclosed air FP cavity was formed as shown in Fig. 1(b), where the lengths of the silica tube and the air cavity are 114 and 90 μm, respectively. The initial length of the air cavity, L_0, at normal pressure, could be controlled by use of silica tube with accurate cleaved-length (an accuracy of < 5 μm can be achieved with the assistance of optical microscope). Figure 2 displays the reflection spectra of air cavities with initial lengths of 44.7, 96.8 and 142.2 μm, respectively, which correspond to the silica tube lengths of ~57, 116 and 151 μm, respectively. The fringe visibility obtained is greater than 15 dB for all the above-mentioned cavities. The fringe visibility would decay quickly with the increase of the air cavity length and for a cavity length of larger than 300 μm, the fringe visibility of less than 1 dB was obtained, owing to the curvature of the air-water interface and the lossy light guidance of the silica tube.

#187405 - $15.00 USD Received 19 Mar 2013; revised 21 May 2013; accepted 25 May 2013; published 5 Jun 2013

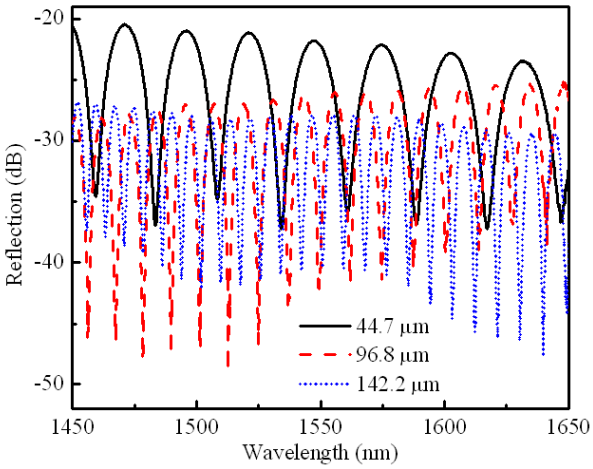

Fig. 2. Reflection spectra of the compressible FP cavities with different initial cavity lengths at normal pressure.

The pressure response of the compressible FP cavity was studied by compressing the air cavities of different initial lengths. Samples were put into a water cell that connected with a nitrogen gas cylinder, and the applied pressure could be adjusted with an accuracy of 0.1 bar. Figure 3(a) shows the reflection spectra of an air cavity ($L_0 = 411\,\mu m$) at 1.5, 3.0 and 5.0 bar, respectively. It can be found from Fig. 3(a) that the fringe visibility can be enhanced by increasing the applied pressure. The cavity lengths and the free spectral range (*FSR*) under different pressures are plotted in Fig. 3(b). An averaged pressure sensitivity of 3.04 μm/kP is obtained between 1 and 1.5 bar, which is nearly two orders of magnitude higher than that of the most sensitive diaphragm-based fiber-tip sensor reported recently [19]. The pressure sensitivity can be further increased by employing an air cavity with longer initial length. The cavity length variation with pressure change is also demonstrated in Fig. 3(b), where for an air cavity with $L_0 = 1063\,\mu m$, the averaged pressure sensitivity obtained is ~6.9 μm/kPa, between 1.0 and 1.3 bar. Within a higher pressure range such as 9~10 bar, the averaged sensitivity is ~161 nm/kPa, much higher than that achieved in state-of-the-art.

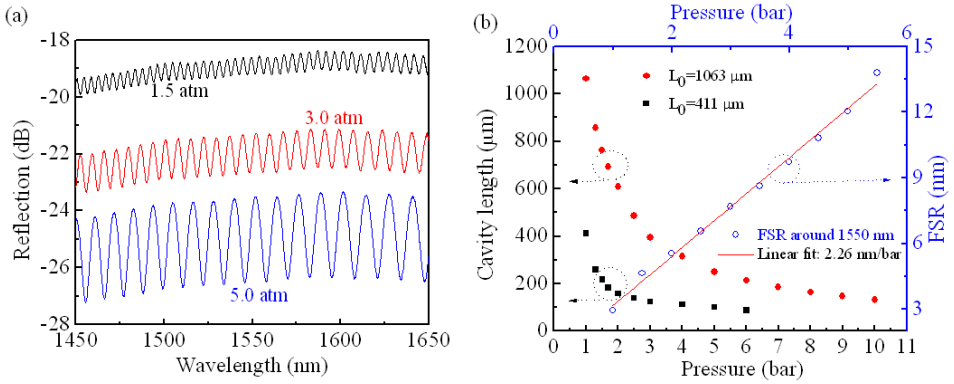

Fig. 3. (a) Reflection spectra and (b) cavity length and FSR of a compressible FP cavity with $L_0 = 411\,\mu m$ under different pressures. The spectra are offset with 2 dB in (a).

It should be noted that while the pressure sensitivity responses nonlinearly to the environmental pressure change, the *FSR* of the interference pattern and the pressure employed exhibit a linear relationship. The FSR of the interference pattern at certain wavelength λ is

#187405 - $15.00 USD Received 19 Mar 2013; revised 21 May 2013; accepted 25 May 2013; published 5 Jun 2013

given by $FSR = \lambda^2 / 2L$. By use of Eq. (1), the sensitivity of FSR to the pressure change in an isothermal process can be derived as:

$$\frac{d(FSR)}{dP} = \frac{\lambda^2}{2P_0 L_0} \tag{3}$$

which is only dependent on the inspected wavelength, λ . For $P_0 = 1$ bar and $L_0 = 411$ μm, the calculated sensitivity of FSR to the pressure change is ~2.92 nm/bar, which is in good agreement with that obtained in the experiment, i.e. 2.26 nm/bar, as shown in Fig. 3(b).

The pressure sensitivity can also be defined as the wavelength shift induced by the pressure change. The dip wavelength of the FP interference fringe is given by: $\lambda = 4\pi L / [(2m+1)\pi - \varphi_0]$, where m is a nonnegative integer and φ_0 is the initial phase. According to Eq. (1), the pressure sensitivity can be derived as:

$$\frac{d\lambda}{dP} = -\frac{\lambda}{P} \tag{4}$$

which implies that the sensitivity is independent of cavity length. Thus for an FP cavity of any length, the sensitivity is −15.5 nm/kPa at 1550 nm under normal pressure. Hence the static pressure measurement accuracy can be calculated to be ~0.65 Pa by assuming a 10-pm wavelength resolution of the optical spectrum analyzer.

An air cavity with $L_0 = 113.3$ μm was sealed into a pressure cell and examined between 0 and 4 kPa above the normal pressure. The pressure increment was monitored by an electrical pressure gauge with an accuracy of 0.1 kPa. A number of fringe wavelength dips around 1550 nm are plotted in Fig. 4, where the linear fitting gives the pressure sensitivities of between 15.63 and 22.82 nm/kPa, slightly higher than those of theoretically predicted. This is possibly caused by the curvature of the air-water interface and the collapsing effect of the silica tube in the proximity of the splicing joint, which makes the air cavity to be cone-like shape and more sensitive to pressure than the cylinder-like air cavity.

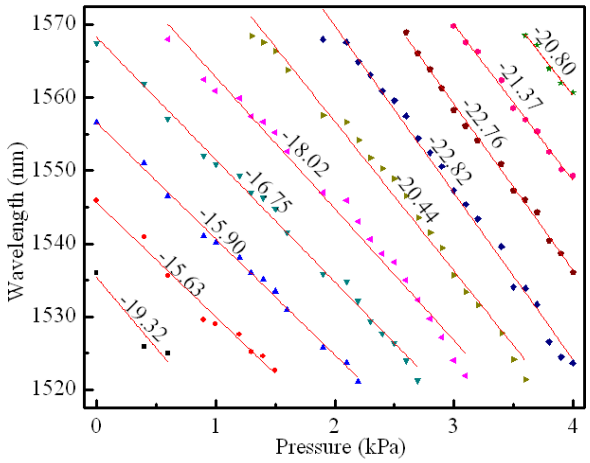

Fig. 4. Dip wavelength shift with pressure change for an air cavity with L_0 =113.3 μm. The labeled values show the pressure sensitivity in nm/kPa obtained by linear fitting.

It should also be noted that external perturbation, such as thermal drifts, may lead to false signals at the sensor readout. The key perturbation for compressible FP cavity is temperature fluctuations. In an isobaric process, the temperature dependence of the proposed sensor can be derived from Eq. (1) as:

#187405 - $15.00 USD Received 19 Mar 2013; revised 21 May 2013; accepted 25 May 2013; published 5 Jun 2013

$$\frac{dL}{dT} = \frac{P_0 L_0}{P T_0} \tag{5}$$

where T_0 is the room temperature, at which the cavity with an initial length of L_0 is formed. By combining Eqs. (2) and (5), the temperature induced cross-sensitivity (S_{TP}) for static pressure measurement is:

$$S_{TP} = -\frac{P}{T_0} \tag{6}$$

By assuming an initial length of $L_0 = 100$ μm and a room temperature of 300 K, the temperature induced cavity length change at normal pressure can be estimated to be ~333 nm/°C according to Eq. (5), and hence the temperature cross-sensitivity can be calculated to be ~0.333 kPa/°C according to Eq. (6), which is slightly lower than that of silver diaphragm-based FPI sensor [19]. For the static pressure measurement with an accuracy of >10 kPa, the pressure measurement error induced by 1°C of temperature-fluctuation could be neglected. Otherwise, temperature must be calibrated to ensure the pressure measurement accuracy.

Despite of the high pressure sensitivity achieved, there are still problems that need to be further investigated, especially for the stabilization of the air bubble and the enhancement of the interference fringe visibility at longer cavity lengths. When used vertically, the air bubble is stable at precise pressure. However, for more versatile applications, the cavity geometry should be optimized by considering the fluid dynamics behavior of water, before a stable air bubble can be maintained. This may be achieved by tapering down the silica tube at the water-entrance, or blocking the silica tube with optical gel at the water-entrance and followed by drilling a microhole by use of femtosecond laser micromachining. The fringe visibility may be enhanced by using liquids of higher refractive index or chemically treated silica tube that exhibits a flat air-liquid interface at longer cavity lengths. Moreover, hollow-core photonic crystal fibers, which exhibit lower transmission loss than that of the silica tube, can also be used to enhance the fringe visibility.

4. Conclusion

In conclusion, we have demonstrated a compressible fiber optic micro Fabry-Pérot cavity for pressure sensing with extremely high sensitivity. By immersing the silica tube spliced at the SMF fiber-tip into water, an air bubble is naturally formed and effectively acts as a micro FP cavity. Such an FP cavity can be compressed by environmental pressure and exhibits a sensitivity of > 1000 nm/kPa at normal pressure, which makes it ideal for pressure and acoustic sensing in gases and liquids. The compressible FP cavity is expected to have potential applications in intracranial pressure measurement, liquid-level monitoring and hydrophone sensing.

Acknowledgments

The authors would like to thank Dr. Jun Ma for helpful discussions. This work was supported by The Hong Kong Polytechnic University research grant 4-ZZE3, and the National Science Foundation of China under grant no. of 61108016.

#187405 - $15.00 USD Received 19 Mar 2013; revised 21 May 2013; accepted 25 May 2013; published 5 Jun 2013